Substantia
An International Journal of the History of Chemistry

Firenze University Press
www.fupress.com/substantia

Research Article

Modeling Social Groups, Policies and Cognitive Behavior in COVID-19 Epidemic Phases. Basic Scenarios.

Franco Bagnoli,[1,2]* Daniele Lorini,[1] Pietro Lió[3]

[1] *Dept. of Physics and Astrophysics, and Center for the Study of Complex Dynamics, University of Florence, Sesto Fiorentino, Italy*
[2] *INFN, Florence section*
[3] *Dept. of Computer Science and technology, University of Cambridge, UK*
*Corresponding author: franco.bagnoli@unifi.it

OPEN ACCESS

Citation: F. Bagnoli, D. Lorini, P. Lió (2020) Modeling Social Groups, Policies and Cognitive Behavior in COVID-19 Epidemic Phases. Basic Scenarios. *Substantia* 4(1) Suppl. 1: 914. DOI: 10.13128/Substantia-914

Received: Apr 21, 2020

Revised: Jun 05, 2020

Just Accepted Online: Jun 11, 2020

Published: Jun 11, 2020

Copyright: © 2020 F. Bagnoli, D. Lorini, P. Lió. This is an open access, peer-reviewed article published by Firenze University Press (http://www.fupress.com/substantia) and distributed under the terms of the Creative Commons Attribution License, which permits unrestricted use, distribution, and reproduction in any medium, provided the original author and source are credited.

Data Availability Statement: All relevant data are within the paper and its Supporting Information files.

Competing Interests: The Author(s) declare(s) no conflict of interest.

Abstract. The covid19 pandemic is distinct from Spanish flu of 1918 from many aspects among which the contrast between the overabundance of worldwide exchange of information (infomedia) and the actual scarce knowledge of the pathogen and the infection mechanism. Another important distinction is that the epidemics threaten society components, social groups, communities and jobs in very different ways and different death tolls. With this in mind, we start with simple models of pandemics and we drive the reader to more complex models that take into accounts social compartments and communities. The discrete-state models are built by adding elements, first in a mean-field approximation, then adding age classes and differential contact rates, and finally inserting the social group dimension. The novel element we insert is the effect of restrictions in contacts and travels, filtered by the risk perception, according with the growth of the number of infected or recovered people. Assimilating risk perception with cognitive behavior, we obtain several coarse-grain scenarios, that can be used for instance to calibrate the level of restrictions so not to exceed the capacity of the health system, and to speed the post-emergency recovery.

Keywords. Epidemic modelling, infection dynamics, risk perception, agent-based models

1. Introduction

The COVID-19 is an infectious disease caused by the Severe Acute Respiratory Syndrome Coronavirus 2 (SARS-CoV-2). (1) The virus is most contagious during the first three days after symptom onset, although spread may be possible before symptoms appear and in later stages of the disease (2). Time from exposure to onset of symptoms is generally between two and fourteen days, with an average of five days (3). The infectivity of the virus is quite high, one person generally infects two to three others (4). At present there is no vaccine available.

The infection's outcome strongly depends on age. Toddlers and teenagers get easily infected but are almost 100% spared from the effects: they are asymptomatic; youngsters (up to 39 years old), could mistype it as common influenza. People in their forties, could find it an ultra-tough influenza. Older people may get pneumonia and could progress to multi organ failure (5) (6), especially in case of co-morbidity (7). Figure 1 shows a representative death toll

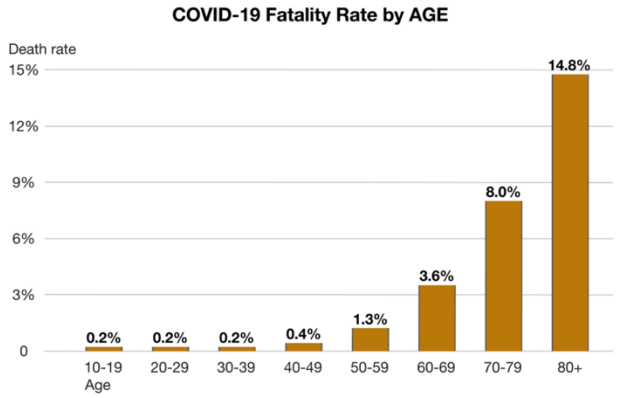

Figure 1. Case fatality rates by age group in China. Data through 11 February 2020.

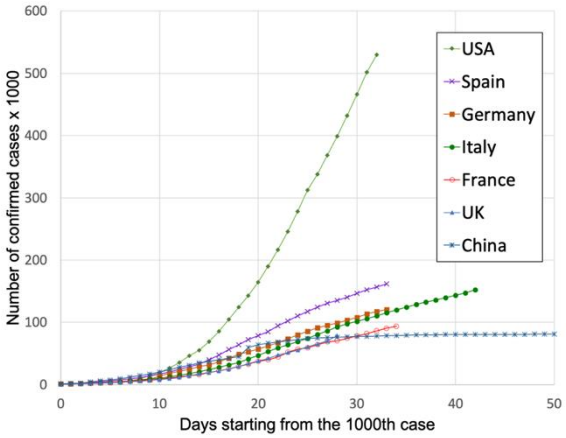

Figure 2. Number of confirmed cases aligned to the 1000th case (11).

distribution by age. Due to the media coverage we may expect that the risk perception for the infection to follow closely this distribution.

There is also a substantial ethnic difference, not related to biological factors. For example, African Americans are dying in larger numbers than white people, particularly in many big USA cities as a result of differential access to medical care (for example mechanical ventilators). At the time of writing, it looks that the mortality is larger in those cities (and continents, such as Africa) with an overloaded health system or with very low density of ICUs (Intensive Care Units) as a result of decades of budget cuts or chronic lack of funding.

Many developed countries have population distribution largely skewed towards middle and older ages. From one side, older ages are correlated to higher probability of needing intensive cares, from the other middle and older ages need more frequently hospitalization in case of infection. The combined effects of these two factors, coupled to the limited number of hospital beds per capita results in severe limitations in handling the sudden spike in the number of COVID-19 hospitalization. The infection initial growth curves for several countries at the date of 12 April 2020 are shown in Fig. 2.

The curves are influenced by the social (contacts) and cognitive behaviors of the groups. For example, elderly people often live together in halls and special structures and may be exposed to higher probability of contagion, unless special precautions are observed. On the other hand, as we shall see in the following, individual behavior (protective habits, avoidance of contacts) can deeply influence the evolution of the disease.

The limited bed per capita capacity and the need for specialized nurses and doctors are significant drivers of the need to flatten the curve (to keep the speed at which new cases occur and thus the number of people sick at one point in time lower). One study in China found 5% were admitted to intensive care units, 2.3% needed mechanical support of ventilation, and 1.4% died (8).

Around 20–30% of the people in hospital with pneumonia from COVID19 needed ICU care for respiratory support (9). The extensive sampling of Vo (10) shows that about 43% of infected people are asymptomatic and 17% needed ICU recovery.

It is noteworthy that the incubation period for COVID-19 is typically five to six days but may range from two to 14 days. A fraction of 97.5% of people who develop symptoms will do so within 11.5 days of infection. This and the large number of asymptomatic infected make the counts of infected people extremely difficult.

The occurrence of the intergenerational caring and the need pf protecting middle-age and elder people has urged the adoption of lockdown practices, thus causing an immediate arrest of the economy and industrial activities. The crucial point for the human species to return to the past lifestyle and avoid millions of deaths is to flatten the curve of infection. Worldwide measures of restriction of contacts, which can take the form of compulsory or voluntary quarantine have been taken by national governs. The main criticism has focused on the rapid decay of national and world economies.

Another important factor is the self-restraint and self-quarantine, induced by the perception of risk of contracting the infection and/or of infecting others. It is noteworthy for instance that the first Chinese patients in the Spallanzani hospital in Rome (the 30th of January 2020) always wore their masks (also before showing any symptoms) and did not infect any other participant of their journey through Italy. Similarly, in spite of the huge return to their families in the South of Italy of people escaping from the forecasted quarantine in the North Italy (around the 21st of February 2020), very few cases appeared in the South, possibly due to a self-imposed quarantine, or at least to a careful obedience to imposed restrictions. Finally, the spreading of the virus in Lombardy is mainly due to the concentration of ill people in hospitals without the proper isolation, a fact that corresponds also to a huge infection rate and mortality among the local medical personnel.

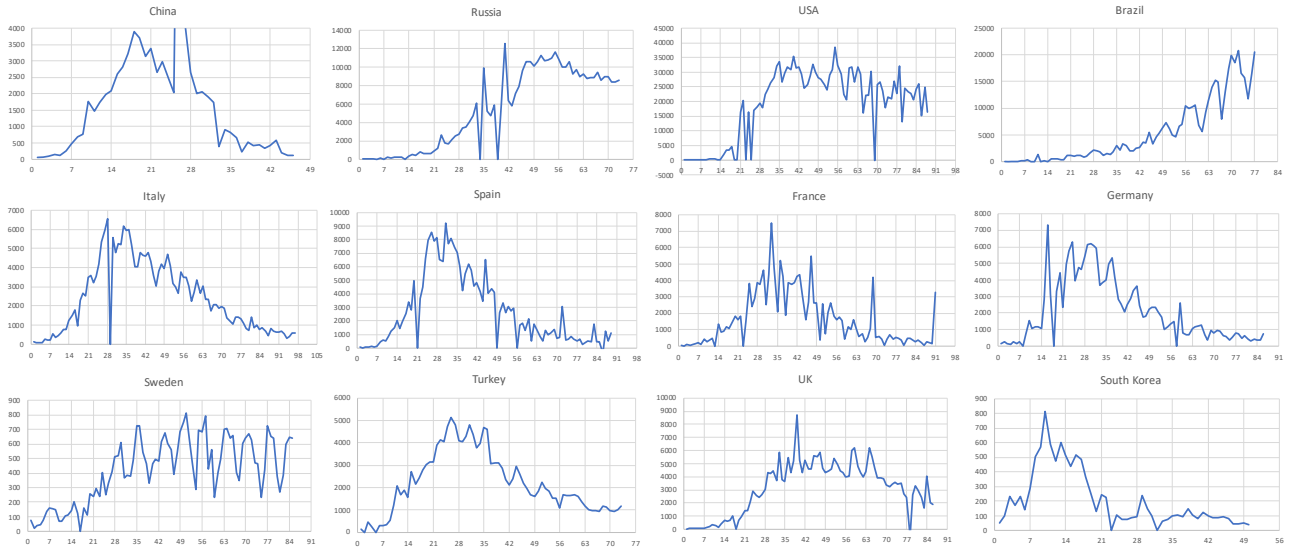

Figure 3. Patterns of daily confirmed cases in different countries/regions starting from the 100th case (12). Data retrieved the 29th May 2020. The horizontal scale is in unit of 7 days to put into evidence the weekly oscillations. Notice that in many cases there in an evident effects of data collection, for instance in Chine there is a jump to 16,000 cases in one day (out of scale), and in Russia there is twice an evident one-day shift of data so that the data jumps to zero are followed by a peak due to the shift. This occurs also in France while in Germany there is a possible anticipation (due to ill-registration) of data. In other countries (Italy, Spain) this shift also occurs, but without the subsequent peaks. However, in many cases there are many variations that cannot be ascribed to data shifts, since they occur over many days. There is often an evident weekly pattern, although not always so regular to be ascribed to data collection.

Models are needed to forecast the progression of the disease and the effects of countermeasures. Most models are based on continuous dynamics, i.e., mean-field, as described in the Section 2, with parameters adapted so to fit average data. However, such models cannot reproduce the sawtooth patterns seen in experimental data (see Fig. 3), and in general do not include the explicit dependence of restriction measures with the progression of the disease. In many cases indeed the patterns in Fig. 3 show a weekly oscillation, which however cannot be ascribed to insufficient data collection during weekends, since the oscillation are not so regular, they span several days and not just the weekend, and the subsequent peak (due to delayed report of data) are not evident. One possibility could be that data not collected/transmitted during weekends are incrementally passed to subsequent days till Friday, but it is improbable that this habit be so widespread in the world. Another possible factor is that there is a weekly contact pace, for instance due to work contacts, that diminishes during weekends and increases the infection rate during workdays.

In general, the simplest infection model says that the infection can stop only if the average number of new infections per each infectivity individual should be less than one. Given the bare infectivity probability τ (for the all duration of the infectivity period) and the average number of contacts $\langle k \rangle$, in the absence of immune people, we have to reduce the product $\tau\langle k \rangle$ (better, $\tau\langle k^2 \rangle / \langle k \rangle$, which is generally similar to $\tau\langle k \rangle$ for uncorrelated networks (13)) to less than one. This can be done either using protective means (like masks, washing hands) which have the effect of reducing τ, or isolation, i.e. reducing $\langle k \rangle$.

In any case, the pre-pandemic high connectivity of humans (implying both the number of contacts and the mobility) constituted an important factor for the spreading of any disease. It can be shown that for scale-free networks (that show a diverging second moment of the connectivity) the epidemic threshold (the critical value of τ) is zero, i.e., no epidemics can be stopped without restrictions to contacts (13).

The effects of the risk perception on the mitigation of an epidemics has been introduced in Ref. (14), and studied in Refs. (13) (15) (16) (See also Ref.(17)) and it has been shown that for networks with finite connectivity (and finite second moment of it), there is always a value of the perception able to stop the epidemics though self-restrictions, but for scale free networks, additional precautions has to be taken by hubs, i.e., people with high connectivity like physicians.

However, the other important ingredient is that the risk perception has to be really given by the actual community of real contacts. What happens is that the information contact network can be quite different from the real one (18), and clearly in this case one can either underestimate the risk, as in Lombardy, or overestimate it, which is harmless unless the over-restrictions then lead to breakage of the norms.

Finally, data from China, Italy and France are best fit by a power-law (19), which is not consistent with the standard mean-field models. This ingredient can be inserted as a phenomenological factor in such models (20).

In this work we present some models incorporating the risk perception and/or the dependence of restriction measures on the number of cases, the presence of several age classes and

finally the geographic distribution. This model cannot be used to fit existing data, due to the great number of parameters (and the lack of an extensive investigation on them) but may be useful for visualizing some possible scenarios.

2. Modelling epidemics

Most of "classical" epidemics models are based on differential equations, but this approach has several "hidden" assumptions, so let us start from the very basics.

In principle, the most accurate model is that in which each individual in a real population is represented by an "agent" in the computer simulation. Clearly, we have to simplify drastically the representation of a person. First of all, we can assume that the state X_i of an individual i can assume a certain number of values, say susceptible (S), infected (I) and, if the disease confers immunity, recovery/refractory (R), i. e., the SIR model. Other common models include also an exposed/asymptomatic (E) state (SEIR model) and can distinguish between actual recovered people and dead ones (the SEIRD model).

Given these states, we have to specify the unit of time for which there can be a transition among states; it is quite natural to assume a time unit of one day, since the reports are issued on a daily base. We should then define the probability of the transition from one state to another, which can depend on the state of other people (as in the case of an infection), or on the previous state of the individual. For accurately modelling the infection phase, one could add intermediate steps, like $I_1, I_2, \ldots$ so that one can avoid the appearance of improbable recovering after a too short period.

For what concerns the infection phase, we should consider the network of contacts of individual i, which can be conveniently defined by a matrix A_{ij}, which gives the probability of a daily contact between individual i and j. Actually, the matrix needs not to be symmetric, since it expresses the modulation of infectivity of individual i from individual j, and this depends on the precaution adopted. The matrix A_{ij} can replicate the fact that intimate (family) connections are stronger, followed by those among the own community, etc., and can also reflect the job or the age class of individual i, so that for instance a teacher or a physician (but also an adolescent) may have more (and more intense) contacts than a retired elder individual.

So, the simplest SIR model for one individual i can be expressed as in Fig. 4, where $[\cdot] = 1$ if $\cdot$ is true and zero otherwise, α is the "bare" infection probability and ε is the recovery probability. A healthy $X_i = S$ individual has a $1-\alpha$ probability to remain in its state following a contact with an infectious person (recovered ones do not convey any more the disease) and α probability to be infected. If infected, he/she has $1-\varepsilon$ chance of remaining in the infected state and ε of healing.

This model can be extended by adding more states, like asymptomatic exposed E, mild symptoms M, people in therapy T, dead individuals D, etc. One can also add age classes, so that susceptibles, for instance, can be in state S_k, where k identifies the class, and can pass to state I_k with probability proportional to α_k, etc.

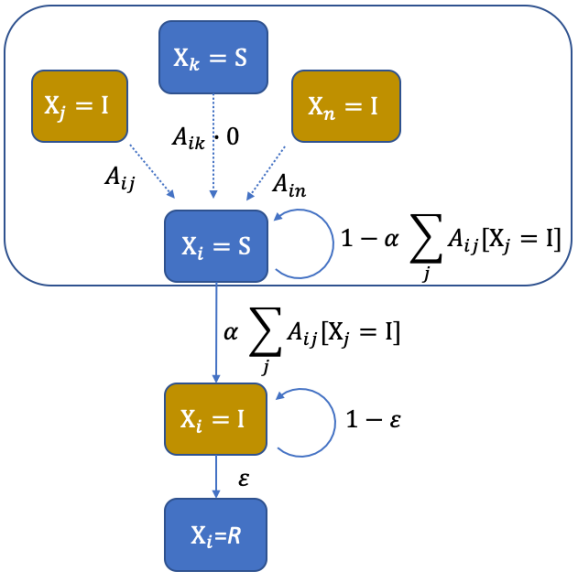

Figure 4. Simple agent-based SIR model

Clearly, this model requires many parameters and is not susceptible by analytic treatment. So, before computers, scholars imposed a "mean-field" or "chemical" assumption, implying homogeneity and isotropy. With these assumptions, one can introduce the probability S of staying in state S (susceptible), I of staying in state I (infective) and R of staying in state R (Refractory), i.e., for a population of N individuals,

$$S = \frac{1}{N}\sum_i [X_i = S].$$

Indicating by K the average connectivity

$$K = \frac{1}{N}\sum_{ij} A_{ij},$$

one gets the following discrete-time equations (for the SIR model)

$$S(t+1) = \big(1 - \alpha K I(t)\big) S(t);$$
$$I(t+1) = (1-\varepsilon) I(t) + \alpha K S(t) I(t);$$
$$R(t+1) = R(t) + \varepsilon I(t);$$

and $S + R + I = 1$. Finally, assuming continuous time, one can convert the previous equations into differential ones.

3. Our model

The models are based on discrete states of individuals. In the first version (Fig. 5) we have 7 states, which correspond in principle to observable quantities:

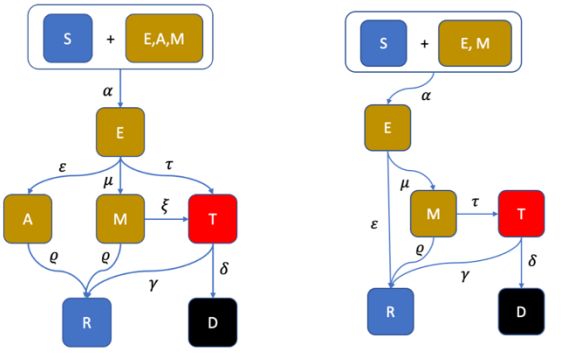

Figure 5. (left) Model-A, 7 states. (right) Model-B, 6 states

S: susceptible;
E: exposed (infectious but yet asymptomatic);
A: asymptomatic (otherwise like E);
M: mild symptoms;
T: therapy (intensive);
D: dead;
R: recovered (heal);

where α, ϵ, μ, τ, ξ, ρ, γ and δ are the transition probabilities on a daily base, and K is the average number of contacts per agent. In order to simplify a bit the model, and also due to the difficulties of detecting asymptomatic people, we can include them into the exposed, and fusing together the probabilities τ and ξ, getting the model-B of Fig. 5, so that we have

ϵ : probability of going from E to R (healing from asymptomatic state);
μ : probability of passing from E to M (inverse of the incubation time);
τ : probability of passing from M to T (aggravation);
δ : probability of passing from T to D (death);
γ : probability of going from T to R (healing with therapies);
ρ : probability of recovery from mild symptoms.

3.1 Estimation of the range of probabilities

We have to estimate the daily probabilities, knowing that the average time $\langle t \rangle$ is related to the probability p by $\langle t \rangle = 1/p$. Obviously ϵ is not known, but we have that $\alpha = 1 - \mu\tau$. In the following, we shall extend the model to different classes of people, either based of their age or on their profession.

The probability of infection (transition $E \to A$) is given both by the fraction of infected (E and/or M, according with the class of people considered) and by the number of contacts per day (that can depend on the age class) K.

Given that α is the probability of infection by one contact, indicating with X the probability that a neighbor is infected, we have on average KX infected neighbors and therefore the probability of not becoming infected is $(1 - \alpha)^{KX}$ and that of becoming infected is $1 - (1 - \alpha)^{KX} \simeq \alpha KX$ if α is small.

If K and X are constant, the average time $\langle t \rangle$ to contract the infection is $\langle t \rangle = 1(\alpha KX)$ and therefore $\alpha = 1(\tau KX)$.

An infected individual surrounded by healthy people can infect in average $n \simeq \alpha K$ people per day ($n \simeq (1 - X)\alpha K$), so if the infectivity period (the quarantine) is $Q \simeq 14$ days is, roughly, $n \simeq \alpha KQ$. If n is about 2.5 and taking for K a value of about $K \simeq 10$, we have $\alpha = \simeq 0.2$.

If we now combine the two formulas, assuming that $\tau \simeq 2$, we have that the fraction of infected individuals (among those exposed) should be $X \simeq 1(2n)$ or approximately the 20%.

Since the probability of remaining in state E is $1 - (\epsilon + \mu)$, assuming that the incubation time is about $w = 7$ days, we have $\epsilon + \mu = 1$. The probability ϵ should be about the inverse of children's recovery time, say $\epsilon \simeq 1/10$. The incubation period is about 5 days, but this is not related to $1/\mu$, since this parameter is rather the probability of showing symptoms.

All probabilities are obviously positive and less or equal to one, and

$$\begin{aligned} \varepsilon + \mu &\leq 1 \\ \gamma + \delta &\leq 1 \end{aligned} \qquad (1)$$

4. Mean-field equations

In the following we shall indicate with the same symbol (italic) the fraction of agents in a given state or, in for the stochastic version, the probability of finding an agent in such state.

The discrete-time equations, essentially equivalent to the Euler scheme for solving differential equations with $\Delta t = 1$, are

$$\begin{aligned} E(t+1) &= (1-\varepsilon-\mu)E(t) + S(t)K(E(t),M(t))X(t); \\ M(t+1) &= (1-\rho-\tau)M(t) + \mu E(t); \\ T(t+1) &= (1-\delta-\gamma)T(t) + \tau M(t); \\ R(t+1) &= R(t) + \varepsilon E(t) + \rho M(t) + \gamma T(t); \\ D(t+1) &= D(t) + \delta T(t); \\ S(t) &= 1 - (E(t) + M(t) + T(t) + R(t) + D(t)). \end{aligned} \qquad (2)$$

The system is linear except for a quadratic nonlinearity in the first equation.

The quantity $K(E,M)$ denotes the average number of contacts of an agent. In the following, we shall let K decrease according to the restriction strategies and perception of the risk, i.e., on the fraction of infected or recovered people. The quantity X denotes the probability of meeting infected people who can spread the disease, so either $X = E$ or $X = E + M$, according with the prevention measures applied to segregate manifestly infectious people.

All simulations start with a small fraction $E(0) = E_0 = 10^{-6}$ of infected people.

Simulations show, as expected, the classic SIR behavior, with the number of susceptible people going to zero, people

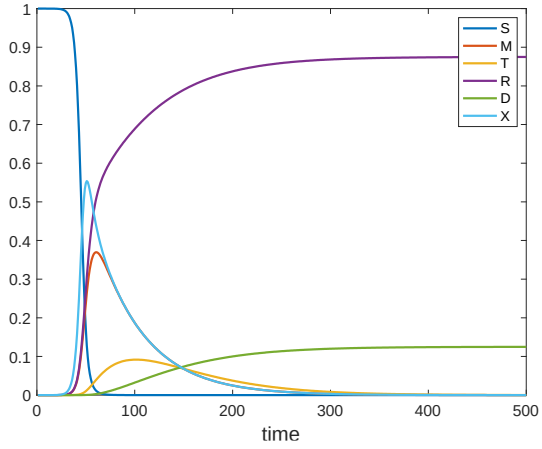

Figure 6. Simple SEIR model, $K = 22$, $\alpha = 0.02$, $\epsilon = 0.1, \mu = 0.1$, $\tau = \delta = \gamma = \rho = 0.01$. Here and in the following figures, time is in days (iterations).

in therapy showing a peak and the deaths reaching a certain final fraction of the population (Fig 6).

In the following we monitor the final fraction of deaths $D_\infty = 0.125$ and the maximal fraction of people in therapy $M_{MAX} = 0.09$, for the simulation of Fig. 6. These values applied to the world population would imply over 900 million deaths and 675 million hospitalized. Applied to the Italian population they would mean 7.5 million dead and 5.4 million hospitalized.

5. Effects of restrictions and/or risk perception

Now let's insert the effect of the restriction measures and/or the perception of the risk, modelled through the decrease of the connectivity K with the number of infected people E, or of people in therapy M.

We assume that the connectivity K is given by the sum of a fixed component K_0 (family) and a variable term K_V, as

$$K(Y) = K_0 + K_V \exp(-cY) \qquad (3)$$

with a new parameter c. We assume that the connectivity decreases with the number showing mild symptoms ($Y = M(t)$), but with the increasing of sampling, it might depend on the number of detected asymptomatic ($Y = E(t)$).

By increasing c to 10, we observe a decrease in connectivity in correspondence with the peaks of people in therapy (Fig. 7-right), with a final fraction of deaths $D_\infty = 0.124$ (almost unchanged), but a maximal fraction of people in therapy $M_{\mathrm{MAX}} = 0.07$, for the simulation of Fig. 7.

By further increasing c (i.e., with much stronger restriction measures) and letting K_V depend on E (implying extended sampling of asymptomatic people), we get a smaller number of $M_{MAX} = 0.02$, at the cost of a longer emergence phase (the timescale is roughly six times in Fig. 8 with respect to Fig. 6). The fraction of deaths has not changed much ($D_\infty = 0.12$) but now not all susceptible people got infected $S_\infty > 0$ (Fig. 8). This is not the same as herd immunity, since the susceptible people can be re-infected once that K has grown again.

Another interesting effect of the risk perception is that the curve of infected people, which in the SEIRD model shows an exponential growth and decrease (Fig. 9-left), with risk perception starts showing a different behavior (Fig. 9-right).

6. Age classes

Different age classes have both different susceptibility, different contact patterns and, moreover, different probabilities of showing symptoms.

We start defining three age classes: young (0-25 y), middle age (25-65 y) and elders (> 65). From the census 2019 in Italy, we get that the respective percentages are 23%, 54% and 23% (21). All parameters now carry an index k, k = 1,2,3 for young, middle age and elder, resp.

$$\begin{aligned}
E_k(t+1) &= (1-\varepsilon_k-\mu_k)E_k(t) + S_k(t)X(t);\\
M_k(t+1) &= (1-\rho_k-\tau_k)M_k(t) + \mu_k E_k(t);\\
T_k(t+1) &= (1-\delta_k-\gamma_k)T_k(t) + \tau_k M_k(t);\\
R_k(t+1) &= R_k(t) + \varepsilon_k E_k(t) + \rho_k M_k(t) + \gamma_k T_k(t);\\
D_k(t+1) &= D_k(t) + \delta_k T_k(t);\\
S_k(t) &= 1 - (R_k(t) + M_k(t) + T_k(t) + R_k(t) + D_k(t)),
\end{aligned} \qquad (4)$$

The equations are coupled by the fraction of infected people $X(t)$

$$X(t) = \sum_k K_k(t)E_k(t).$$

For beginning, we used the set of parameters of Table 1

Table 1. set of parameters of the age-class model of Eq. (4).

parameter	young	middle age	elders
α	0.02	0.02	0.02
ϵ	0.1	0.01	0.001
μ	0.0	0.01	0.1
τ	0.0	0.01	0.1
δ	0.0	0.001	0.01
γ	0.0	0.001	0.02
ρ	0.01	0.01	0.01
K_V	20	20	4
K_0	2	2	1
c	c_0	c_0	c_0

As expected, with a small value of $c_0 = 1$, little changes for the total values (although not all susceptibles now get infected), but the distribution for the different age classes are obviously different (and the most of infected came from middle age), Fig. 10. However, even for limited risk perception, the number of deaths seems to follow a curve similar to a power-law, as in real data (19). The final fraction of deaths is $D_\infty \simeq 0.067$ and the maximum fraction of people in therapy is $M_{\mathrm{MAX}} \simeq 0.08$.

For larger values of c_0 (100), as in the previous case the epidemics lasts longer, but the numbers $M_{\mathrm{MAX}} \simeq 0.017$ and $D_\infty \simeq 0.059$ lower, and the fraction of susceptibles who do not get infected increases, see Fig. 11.

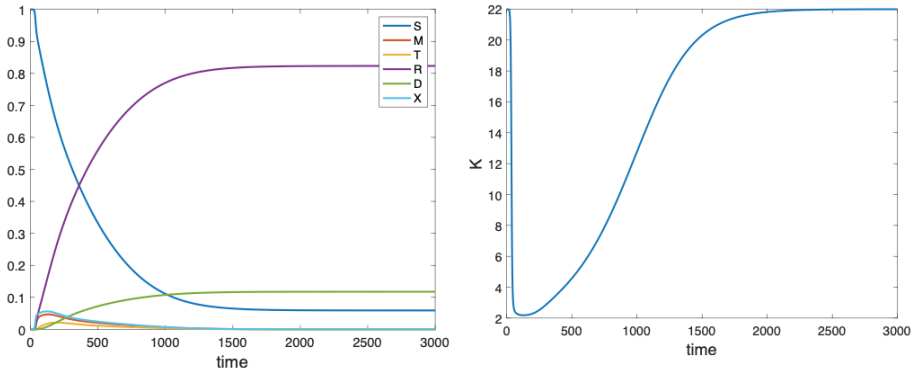

Figure 8. SEIR model with risk perception, $c = 100$, other parameters as in Fig 7. Left: time plot of observables Eq. (2), right: time plot of connectivity $K(t)$, Eq. (3)

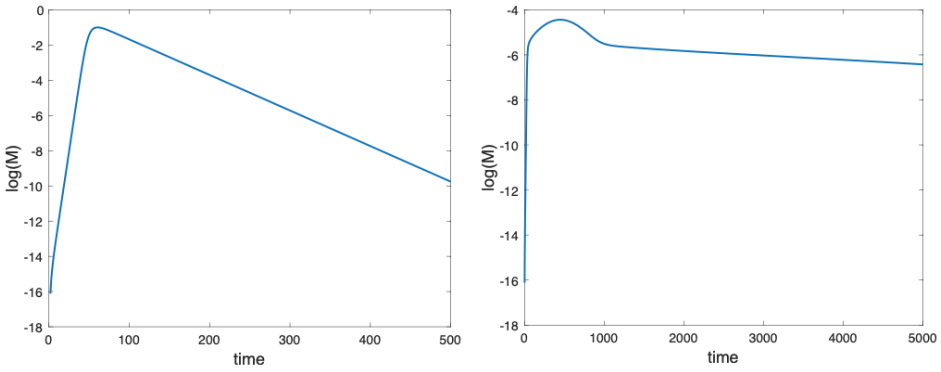

Figure 9. Plots in a log-lin scale. (left) fraction of M people without risk perception ($c = 0$); (right) fraction of M people with extreme risk perception $c = 1000$, other parameters as in Fig 7

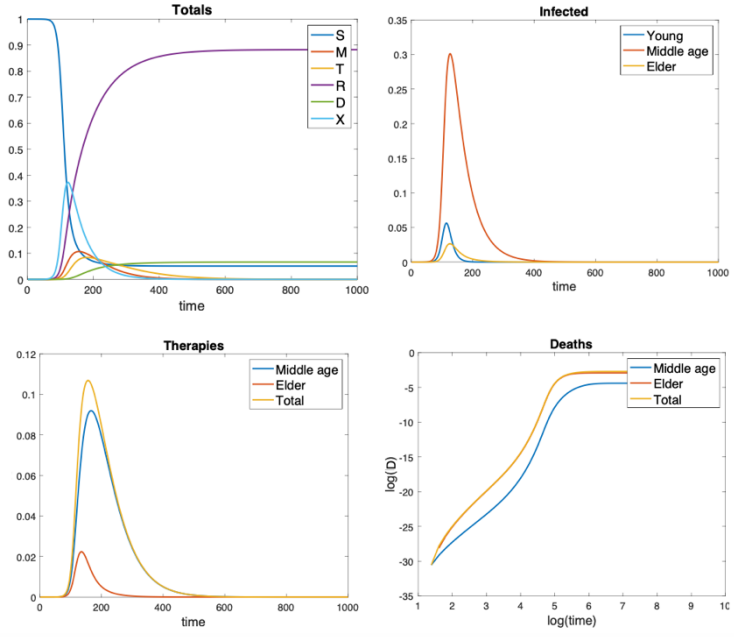

Figure 10. $c_0 = 1$, other parameters as in Table 1. (top left) total fractions; (top right) infected for different age classes; (bottom left) people in therapy; (bottom right) deaths on a log-log scale.

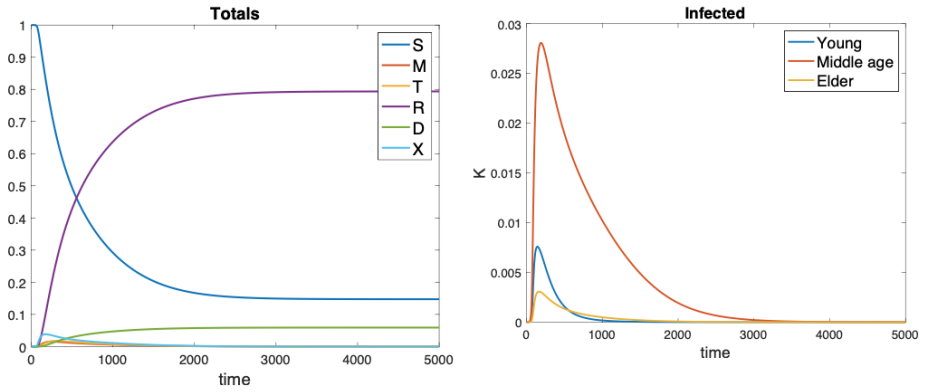

Figure 11. $c_0 = 100$*, other parameters as in Table 1. (top left) total fractions; (top right) infected for different age classes; (bottom left) people in therapy; (bottom right) deaths on a log-log scale.*

7. Social groups model

The main goal of restriction measures is that of stopping the epidemics before it reaches all the country. In order to model it, we need to introduce a spatial model. Let us denote by A_{ij} the probability of contact between individuals i and j. The contact needs not to be symmetric, since the transmission of the disease depends on the precautions taken. We consider a hierarchical network (22), of the type of Fig. 12-left. It is defined by a block matrix I of the type of Fig. 11-right. The index matrix I defines the parameters of the matrix A: $A_{ij} = 1$ with a certain probability $p(I_{ij})$ such that the average number of contacts of an individual in community n is $K^{(n)}$.

The index matrix I is defined by the size L of the blocks, in the example of Fig. 12 they are $L^{(1)} = 2, L^{(2)} = 3, L^{(3)} = 2$ (the size of the smallest community is 2, the following one is composed by 3 smaller communities, and the whole system is composed by 2 intermediate communities). One can think of families, cities and country.

The number of connections may change from individual to individual, when chosen with the realization of the stochastic choice of connections with probability $p^{(n)}$, as in Fig. 12-left, but for simulations it is faster to keep K^n fixed and choose this number of individual at random among the given community. The random choice is repeated in each time step (annealed version) or may be kept fixed (quenched version). The annealed version assures that there is no isolated community, a case that may happen in the quenched version for low connectivity. In the following we use the annealed version.

The matrix A is generated according to I and p's at each time step (annealed), and actually in simulations we do not have any matrix, just the probability of connections that are translated into the number of contacts in each community, randomly chosen.

The equations are the same, but now the connection K is split into that of the different communities, and also the infection rate α depends on the community n, so we have now

$$I = \begin{pmatrix} 1 & 1 & 2 & 2 & 2 & 2 & 3 & 3 & 3 & 3 & 3 & 3 \\ 1 & 1 & 2 & 2 & 2 & 2 & 3 & 3 & 3 & 3 & 3 & 3 \\ 2 & 2 & 1 & 1 & 2 & 2 & 3 & 3 & 3 & 3 & 3 & 3 \\ 2 & 2 & 1 & 1 & 2 & 2 & 3 & 3 & 3 & 3 & 3 & 3 \\ 2 & 2 & 2 & 2 & 1 & 1 & 3 & 3 & 3 & 3 & 3 & 3 \\ 2 & 2 & 2 & 2 & 1 & 1 & 3 & 3 & 3 & 3 & 3 & 3 \\ 3 & 3 & 3 & 3 & 3 & 3 & 1 & 1 & 2 & 2 & 2 & 2 \\ 3 & 3 & 3 & 3 & 3 & 3 & 1 & 1 & 2 & 2 & 2 & 2 \\ 3 & 3 & 3 & 3 & 3 & 3 & 2 & 2 & 1 & 1 & 2 & 2 \\ 3 & 3 & 3 & 3 & 3 & 3 & 2 & 2 & 1 & 1 & 2 & 2 \\ 3 & 3 & 3 & 3 & 3 & 3 & 2 & 2 & 2 & 2 & 1 & 1 \\ 3 & 3 & 3 & 3 & 3 & 3 & 2 & 2 & 2 & 2 & 1 & 1 \end{pmatrix}$$

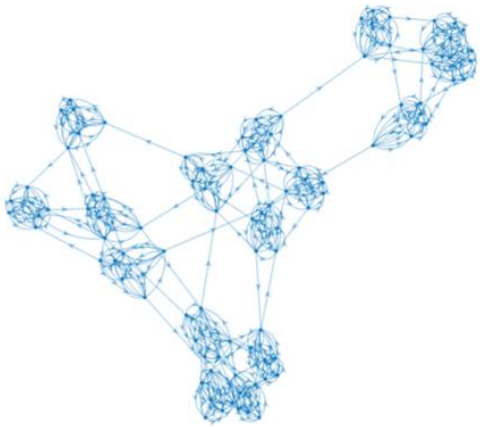

Figure 12. (left) Index of a hierarchical network with three-community sizes $L = \{2,3,2\}$*. (right) A realization of a network with* $L = \{6,4,4\}$ *and connection probability* $p = \{1,0.04,0.002\}$*.*

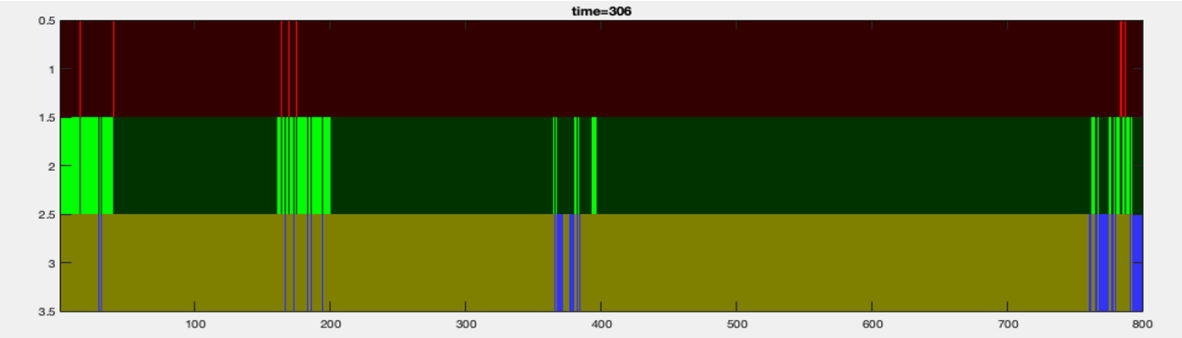

Figure 13. A snapshot of the status of the network. Bottom line denotes susceptible individuals (blue marks infected or recovered or died), middle lines are infected (light green marks), top line represents deaths (red marks).

a real agent-based model (for the moment without age structure).

Let us consider for the moment a simple model with four states: S, E, R and D (SERD) and three parameters: $\alpha^{(n)}$, infection probability from infected people in community n, ρ, recovery rate and δ, death rate.

The transition probabilities of an individual i are

$$
\begin{aligned}
S_i &\to \begin{cases} E_i & \text{with probability } \sum_n \sum_{m=1}^{K^{(n)}} \alpha^{(n)} \left[Q_{j(m)\in L^{(n)}} = E_i \right]; \\ S_i & \text{otherwise;} \end{cases} \\
E_i &\to \begin{cases} R_i & \text{with probability } \rho; \\ S_i & \text{with probability } \delta; \\ E_i & \text{otherwise;} \end{cases} \\
R_i &\to R_i; \\
D_i &\to D_i;
\end{aligned} \tag{5}
$$

where $j(m)$ indicates and individual at random in community m, $Q_{j(m)\in L^{(n)}}$ is its state and again $[\cdot]$ is one if $\cdot$ is true and zero otherwise.

Let us consider for instance the case $L = \{4,10,20\}$ (800 individuals), $K = \{4,2,1\}$ and $\alpha = \{0.8,0.01,0.001\}$, see Fig. 13 and 14-left.

As expected, we see a quick propagation inside a first-level community, followed by sporadic breakdown in other communities, Fig. 13.

The infection curve starts to assume the saw-tooth appearance of those coming from actual data, Fig. 3 and all curved show sudden jumps, Fig. 14-left. If we allow the contacts among communities only during workdays (increasing the inter-community infectivity $\alpha = \{0.8,0.05,0.003\}$), we get a more marked pattern, fig. 14-right.

8. Improvements and perspectives

The models here presented constitute just the first approximations to the problem. First of all, we are developing the spatial model with age classes, and implementing a more real network structure, with quenched and annealed parts, representing the connections that are stable (family, school, some kind of work) and those that are variable (casual contacts, commerce, travels). In this way one can simulate with more efficacy the effects of restrictions and the perspective of reopening. Clearly, these improvements come

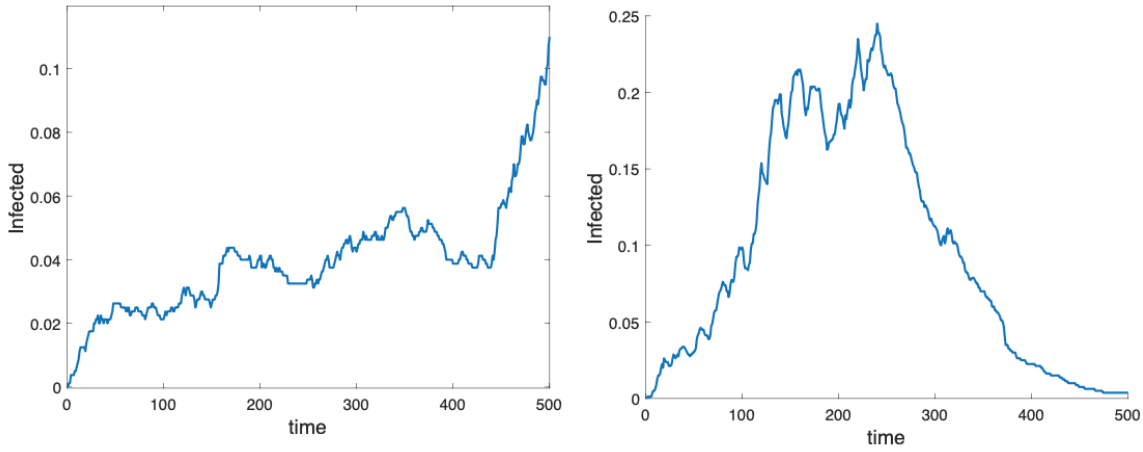

Figure 14. (left) Saw-tooth behavior of infection curve. (right) More pronounced behavior with infection limited to workdays.

at the cost of increasing the number of parameters, which are quite difficult to estimate from field data (often missing and quite sparse).

9. Conclusions

We have presented some basic simulation scenarios for an infectious disease inspired by the observed characteristics of Covid-19. We started with the "classical" mean-field approach based on time-discrete equations, introducing the risk perception effects by means of the restrictions of contacts, and age classes, showing that in this case the overall growth of deaths (and of other quantities) is no more an exponential, but shows a power-law like behavior.

We then introduced an agent-based model, limited to the standard infection case (without age classes and risk perception) showing that the network of contacts organized in communities is a crucial ingredient for reproducing the observed saw-tooth behavior and sudden outbreaks.

Further work is ongoing for developing a unified model, with the goals of furnishing a tool for interpreting the observed scenarios, without any presumption of fitting observed data and forecasting the outcome of the pandemic.

REFERENCES

1. **WHO, World Health Organization.** Naming the coronavirus disease (COVID-19) and the virus that causes it. [Online] 2020. https://www.who.int/emergencies/diseases/novel-coronavirus-2019/technical-guidance/naming-the-coronavirus-disease-(covid-2019)-and-the-virus-that-causes-it.

2. **CDC, Center for Disease Control and Prevention.** *How COVID-19 Spreads.* [Online] Apr. 2, 2020. https://www.cdc.gov/coronavirus/2019-ncov/prevent-getting-sick/how-covid-spreads.html.

3. **Hui, David S., et al.** The continuing 2019-nCoV epidemic threat of novel coronaviruses to global health — The latest 2019 novel coronavirus outbreak in Wuhan, China. 2020, Vol. 91, pp. 264-266.

4. **Politi, Daniel.** WHO Investigating Reports of Coronavirus Patients Testing Positive Again After Recovery By DANIEL POLITI. *Slate.* [Online] 4 11, 2020. https://slate.com/news-and-politics/2020/04/who-reports-coronavirus-testing-positive-recovery.html.

5. **Heymann, Davide L., Shindo, Nahoko, et al. (WHO Scientific and Technical Advisory Group for Infectious Hazards).** COVID-19: what is next for public health? 2020, Vol. 395, pp. 542-545.

6. **Cascella, Marco, et al.** Features, Evaluation and Treatment Coronavirus (COVID-19). 2020.

7. **Palmier, Luigi et al. (COVID-19 Surveillance Group).** *Characteristics of COVID-19 patients dying in Italy.* s.l. : Istituto superiore di Sanità, Italy, 2020. https://www.epicentro.iss.it/en/coronavirus/bollettino/Report-COVID-2019_2_april_2020.pdf.

8. **Guan, Wei-jie Guan et al.** Clinical Characteristics of Coronavirus Disease 2019 in China. 2020.

9. **Center for Disease Control and Prevention.** Interim Clinical Guidance for Management of Patients with Confirmed Coronavirus Disease (COVID-19). *Centers for Disease Control and Prevention.* [Online] 4 6, 2020. https://www.cdc.gov/coronavirus/2019-ncov/hcp/clinical-guidance-management-patients.html.

10. **Lavezzo, E. et al.** *Suppression of COVID-19 outbreak in the municipality of Vo, Italy.* medRxiv 2020.04.17.20053157. 2020. doi: https://doi.org/10.1101/2020.04.17.20053157.

11. **WHO, World Health Organization.** Coronavirus disease (COVID-19) Dashboard. [Online] https://covid19.who.int/.

12. **ECDC, European Centre for Disease Prevention and Control.** COVID-19 Coronavirus data. [Online] 4 12, 2020. https://data.europa.eu/euodp/it/data/dataset/covid-19-coronavirus-data.

13. **Bagnoli, Franco, Lió, Pietro and Sguanci, Luca.** Risk perception in epidemic modeling. 2007, Vol. 76, p. 061904.

14. **Capasso, V. and Serio, G.** A Generalization of the Karmak-McKendrick Deterministic Epidemic Model. *Mathematical Biosciences.* 1978, Vol. 42, pp. 43-61.

15. **Pastor-Satorras, Romualdo, et al.** Epidemic processes in complex networks. 2015, Vol. 87, p. 925.

16. **d'Onofrio, A. and Manfredi, P.** Information-related changes in contact patterns may trigger oscillations in the endemic prevalence of infectious diseases. *J. Theor. Biol.* 2009, Vol. 256, pp. 473–478.

17. **Manfredi, P. and d'Onofrio, A. (editors).** *Modeling the Interplay between Human Behavior and the Spread of Infectious Diseases.* New York : Springer, 2013. ISBN 978-1-4614-5473-1.

18. **Massaro, Emanuele and Bagnoli, Franco.** Epidemic spreading and risk perception in multiplex networks: A self-organized percolation method. 2014, Vol. 90, p. 052817.

19. **Dong, E., Du, H. and Gardner, L.** An interactive web-based dashboard to track COVID-19 in real time. 2020, Vol. 3099, pp. 19-20.

20. **Fanelli, Duccio and Piazza, Francesco.** Analysis and forecast of COVID-19 spreading in China, Italy and France. 2020, p. 109761.

21. **ISTAT.** Popolazione per età, sesso e stato civile 2019. *tuttitalia.* [Online] 1 1, 2019. https://www.tuttitalia.it/statistiche/popolazione-eta-sesso-stato-civile-2019/.

22. **Girvan, Michelle and Newman, Mark E.J.** Community structure in social and biological networks. 2002, Vol. 99, pp. 7821–7826.